The impact of calcination on changes in the physical and mechanical properties of the diatomites of the Leszczawka Member (the Outer Carpathians, Poland)

Beata Figarska-Warchoł[1], Marek Rembiś[2], Grażyna Stańczak[3]

[1]AGH University of Science and Technology, Faculty of Geology, Geophysics and Environmental Protection, Department of Economic and Mining Geology; al. A. Mickiewicza 30, 30-059 Krakow; e-mail: figarska@agh.edu.pl; ORCID ID: 0000-0002-6962-1775
[2]AGH University of Science and Technology, Faculty of Geology, Geophysics and Environmental Protection, Department of Hydrogeology and Engineering Geology; al. A. Mickiewicza 30, 30-059 Krakow; e-mail: mrembis@geol.agh.edu.pl; ORCID ID: 0000-0003-2879-3949
[3]AGH University of Science and Technology, Faculty of Geology, Geophysics and Environmental Protection, Department of Economic and Mining Geology; al. A. Mickiewicza 30, 30-059 Krakow; e-mail: grazyna.stanczak.99@gmail.com; ORCID ID: 0000-0002-6618-5998

Abstract: The work concerned the effects of the thermal treatment of diatomites from the Jawornik deposit (an example of the diatomites of the Leszczawka Member of the Polish Outer Carpathians). Five distinct lithological varieties were subjected to calcination at 600°C in ambient air.

The thermal impact induced the following changes to the rocks. Their overall rock porosity increased, most distinctly in the initially softer varieties, and the internal pores of the siliceous frustules themselves usually became larger due to the initial melting of the silica phases. Most of the diatoms, quartz and feldspars cracked as a result of their brittle fracturing under compressive strain resulting from substantial and differing size changes of growing grains. Clay minerals were thermally transferred, changing their volume. The organic matter dispersed throughout the diatomites was partly oxidized and removed.

At the same time, the structure of the rocks was strengthened, as confirmed by an increase in their microhardness. The microhardness of soft and porous diatomite varieties increased considerably on heating, but that of the hard and compact variety changed to a smaller degree. The increase is directly related to the content of the clay minerals. The impact of other mineral components was not detected.

The calcination of lithologically diversified diatomites provided the mineral with raw material with deicing and antisliding properties. The technology of its production has been determined by the authors and submitted as a patent.

Keywords: silica, thermal modification, scanning electron microscopy, Vickers microindentation hardness, porosity, apparent density, water absorption

INTRODUCTION

Diatomites have exceptional physical properties, including high porosity with small diameters of rock pores and a considerably developed specific surface (Gao et al. 2005), which result in their high permeability (Murer et al. 2000). They are also characterized by a framework composed of grains (mainly diatoms) with very small diameters, low thermal conductivity and low bulk

density. These specific features determine a wide range of the industrial applications of diatomites, such as catalysers, filters and sorbents of various liquids as well as of inorganic and organic chemical substances. Diatomites are also used, e.g. as structural composite fillers, diffraction gratings of optical sensors, additives to some cement types, raw materials for producing water-glass, glaze, paper and medicines (Cummins 1973, Obanijesu et al. 2004, Fustinoni et al. 2005). Advances in the studies on diatomites continuously extend the range of their usage. There have been attempts to manufacture materials with a 3-D structure that emulates the structure of diatoms (Sandhage et al. 2002, Haluska et al. 2005). Chemical transformations of diatomites are conducted to obtain novel materials with unique technological properties (Wu et al. 2005, Li et al. 2007, Xiong & Peng 2008, Yarusova et al. 2012). The sorption properties of diatomites can be improved, among others, modifying the rocks by their calcination in the range 600–1200°C (Goren et al. 2002, Khraisheh et al. 2005, Martinovic et al. 2006, Yılmaz & Ediz 2008, Zhi-Yang et al. 2009, Ediz et al. 2010, Ibrahim & Selim 2010). Considering that diatomites occurring in various lithostratigraphic units which are highly diversified in their lithologies, the properties of these mineral raw materials and the possibilities of their modification should be subject to comprehensive analysis.

Investigations of diatomites in Poland were initiated by J. Kotlarczyk in the 1950s (Kotlarczyk 1955) and followed in the next decades, providing data on petrographical characteristics and assessments of essential, physical properties of these rocks, of their concentrating and utilization (Kotlarczyk 1966, 1988a, 1988b, Russocki 1981, Kotlarczyk et al. 1986, Smoleńska & Rembiś 2002). The results showed that the diatomites from the eastern part of the Outer Polish Carpathians, despite being such unique rocks, have technological properties slightly inferior to those of their counterparts in other parts of the world (Fuya et al. 1995, Aruntaş et al. 1998, Hassan et al. 1999, Abrantes et al. 2007, Mohamedbakr & Burkitbaev 2009). More recent investigations of these rocks (Figarska-Warchoł et al. 2015, Stańczak et al. 2015, Toboła et al. 2015) focused on the relation between their petrographical development and

physical and mechanical properties. The results of previous works have pointed out that the thermal treatment of diatomites from the Polish Carpathians is a promising method to improve some of their properties, which should pave the way for wider technological applications of these domestic raw materials. Such a calcination treatment of the diatomites from Jawornik in the Polish Carpathians was carried out within the framework of the project presented here. Next, the authors focused on establishing the changes to the microstructure and some physical and mechanical properties, including microhardness, of the thermally modified diatomites. The experiments were focused on obtaining diatomites with higher microhardness and porosity that can be used to produce road aggregates characterized by their deicing and antisliding properties. A comparison of the results obtained for several distinguished varieties of the Jawornik diatomites formed the basis to assess a relation between the petrographical features of these rocks and the effectiveness of their calcination. Such investigations are a novelty in the case of diatomites from the Polish Carpathian flysch.

MATERIAL

Location of the diatomites

There are three horizons formed by the diatomites within the profile of the youngest, Oligocene – Lower Miocene flysch strata of the Skole Unit, that occurs in the eastern part of the Polish Outer Carpathians (Kotlarczyk 1982). The lowest horizon, named the Futoma Diatomite Member of the Lower Oligocene age, is located within the lower part of the Menilite Formation (Kotlarczyk & Leśniak 1990, Marcinowski et al. 2011). The middle one is the horizon of the Piątkowa Diatomite dated to the Upper Oligocene – Lower Miocene. It occurs in the lower part of the Strzyżów Formation (previously called the Upper Krosno Beds) within the Niebylec Shale Member (Koszarski & Żytko 1961, Malata 1996). The third, uppermost diatomite horizon is represented by the Lower Miocene (Burdigalian) Leszczawka Diatomite Member, located in the upper part of the Strzyżów Formation (Koszarski & Żytko 1961, Kotlarczyk 1966, 1982, Malata 1996).
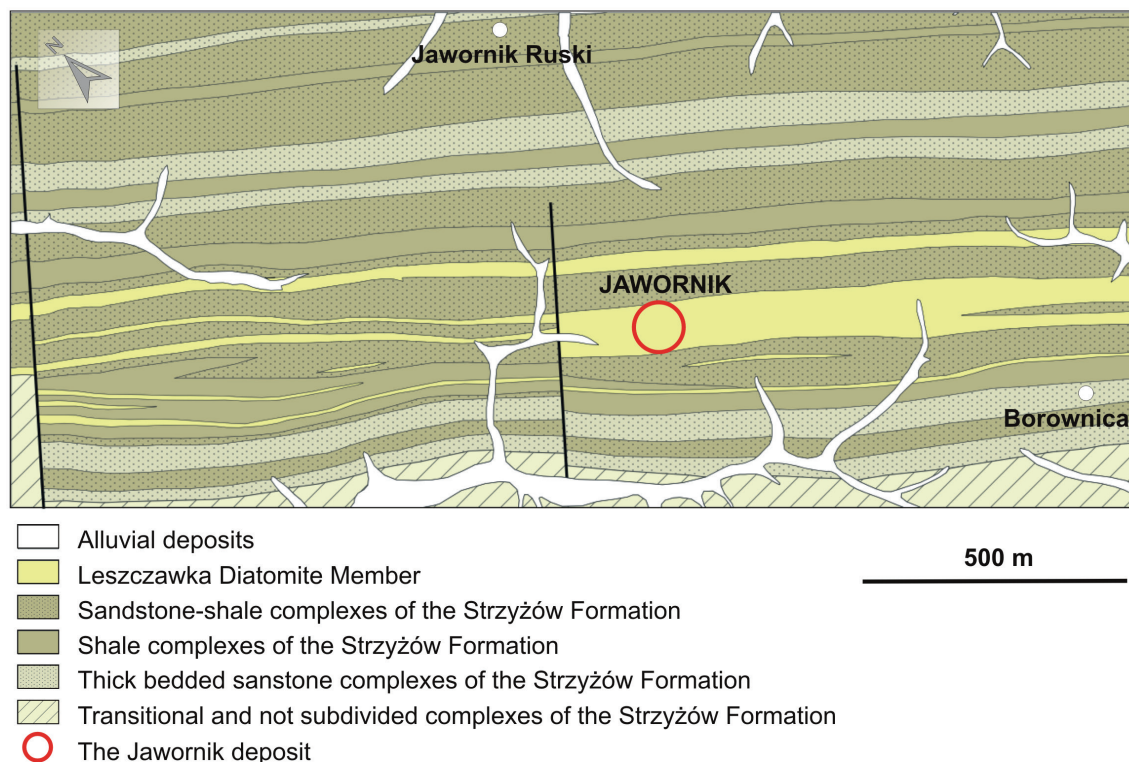
Fig. 1. *Location of the Jawornik deposit on the geological map of the Leszczawka Syncline near Jawornik Ruski after Kotlarczyk (1966, 1988b)*

The strata of these formations are part of a depositional megasequence formed during the last stage of the synorogenic closing of the sedimentary basins in the Polish section of the Flysch Carpathians (Malata & Poprawa 2006, Oszczypko 2008, Szydło et al. 2014). The volcanic activity of that period, manifested by intercalations of pyroclastic rocks, might be the source of the material essential for the development of siliceous sediments, including diatomites (Jucha & Kotlarczyk 1961, Żgiet 1963, Malata & Poprawa 2006, Oszczypko 2008, Szydło et al. 2014).

Within the Leszczawka Member, diatomites occur in axial parts of several synclines, of which the most representative for the horizon discussed is the Leszczawka Syncline. In its north-western part, located near Jawornik Ruski, the diatomite member is separated into three lithosomes, between which the sandstone-shale strata of the Strzyżów Formation rest (Fig. 1). The Jawornik deposit of diatomites from which the samples were collected occurs within the middle lithosome that has the features of an olistostrome (Kotlarczyk 1982, 1988a, 1988b).

Lithological characteristics of the diatomites

The diatomites of Jawornik have colours varying from light creamy to yellowish orange to grey and dark grey. They are microporous and their texture is usually random. Each of the lithological rock varieties disintegrates in a specific way during physical weathering, and the same is observed when breaking bigger blocks into smaller fragments. This rather obvious identifying feature, already mentioned by Kotlarczyk (1966), and rock colour have been accepted as the classification basis of the Leszczawka diatomites and permitted five lithological varieties to be distinguished (Figarska-Warchoł et al. 2015):
1) light creamy diatomites with blocky disintegration (variety BL);
2) dark creamy, grey or dark grey diatomites with blocky disintegration (variety BD);
3) light creamy, dark creamy or light grey diatomites with platy or prismatic disintegration (variety PL);

4) dark grey diatomites with platy or prismatic disintegration (variety PD);

5) yellowish orange diatomites with nodular disintegration (variety N).

The detailed lithological characteristics of these rock types were given by Figarska-Warchoł et al. (2015). The major detrital component is represented by fragmented, less often complete frustules (Tab. 1), with sizes reaching 50–100 μm. Their shapes in optical and scanning electron microscopes may be circular or elongated (elliptic, rhomboidal or crescent). These diatom fossils represent both the marine and the freshwater habitat assemblages which, according to Kotlarczyk (1982), proves the allochtonous origin of their parent sediments. The frustules are porous and reveal a complex internal structure, expressed by the presence of many grooves and small ribs. The content of diatoms in the examined diatomites with the blocky disintegration (varieties BL and BD) is 43.4% and 61.0%, respectively; in those with the platy or prismatic disintegration (varieties PL and PD) 44.8% and 44.7%, respectively; while in those with nodular disintegration (variety N) only 36.0% (Tab. 1). The contents of other detrital components are much lower, as their totals range from 5.3% in the PD variety to 10.1% and 11.6% in the BL and BD varieties, respectively, to 13.0% in the PL variety and 15.3% in the N variety (Tab. 1). They are represented by angular quartz grains, usually several dozen micrometers large, revealing many signs of surface dissolving and less frequent single fractures. Quartz is accompanied by elongated flakes of muscovite, grains of sericitized feldspars (albite-rich), fragmented spiculae of siliceous sponges and accumulations of partly weathered glauconite with sizes reaching 110 μm.

The groundmass of the diatomites is mainly of the porous character and occasionally of the basic one. Its contents range from 31.0% (variety BD) to 50.0% (PD one) (Tab. 1). It is composed of silica of different ordering (opal-A and opal-CT) and clay minerals (illite, kaolinite and smectite) (Figarska-Warchoł et al. 2015). The PD variety is characterized by the highest amorphous silica content of the groundmass (up to 35%) at a considerably lower content of clay minerals (ca. 16%). In the diatomites of the BL variety, the siliceous and clay components of the groundmass occur in comparable amounts (ca. 20–25%), whereas the silica content of the BD and PL varieties is low, not exceeding 10%, and completed with abundant clay minerals. In the groundmass of most of the diatomites, low amounts of iron oxides (1–2%) in the form of fine, automorphic crystals scattered evenly among other minerals usually also occur. It is only the nodular splitting diatomite form (N variety), whose content of iron compounds (16.5%) is considerable. Simultaneously, this variety contains only 9% of silica.

Table 1

Mineral composition [vol.%] of raw diatomite varieties from the Jawornik deposit based on the SEM micrographs

Diatomite variety	Diatoms[1] (complete/ fragments)	Quartz[1]	Other grains[1]				Groundmass[2]			
			Micas	Feldspars	Glauconite	Sponge spicules	Opal	Clay minerals	Iron oxides/ hydroxides	Organic substance
BL	43.4 (44.2/55.8)	6.6	2.2	2.2	1.7	0.7	18.38	22.98	0.92	0.92
BD	61.0 (35.6/64.4)	5.4	1.5	0.5	0.3	0.3	3.93	22.70	0.87	3.49
PL	44.8 (27.3/72.7)	8.0	2.6	1.9	0.3	0.2	7.03	31.21	1.76	2.20
PD	44.7 (17.9/82.1)	3.4	1.0	0.6	0.3	0.0	32.08	15.57	0.94	1.42
N	36.0 (33.6/66.4)	6.7	3.4	3.9	1.3	0.0	7.65	23.34	13.28	4.43

Explanations: The values are results (1) of measurements based on the SEM micrographs and (2) of estimation made on the basis of chemical and microscopic rock analyses. Other grains = total of micas, feldspars, glauconite, sponge spicules
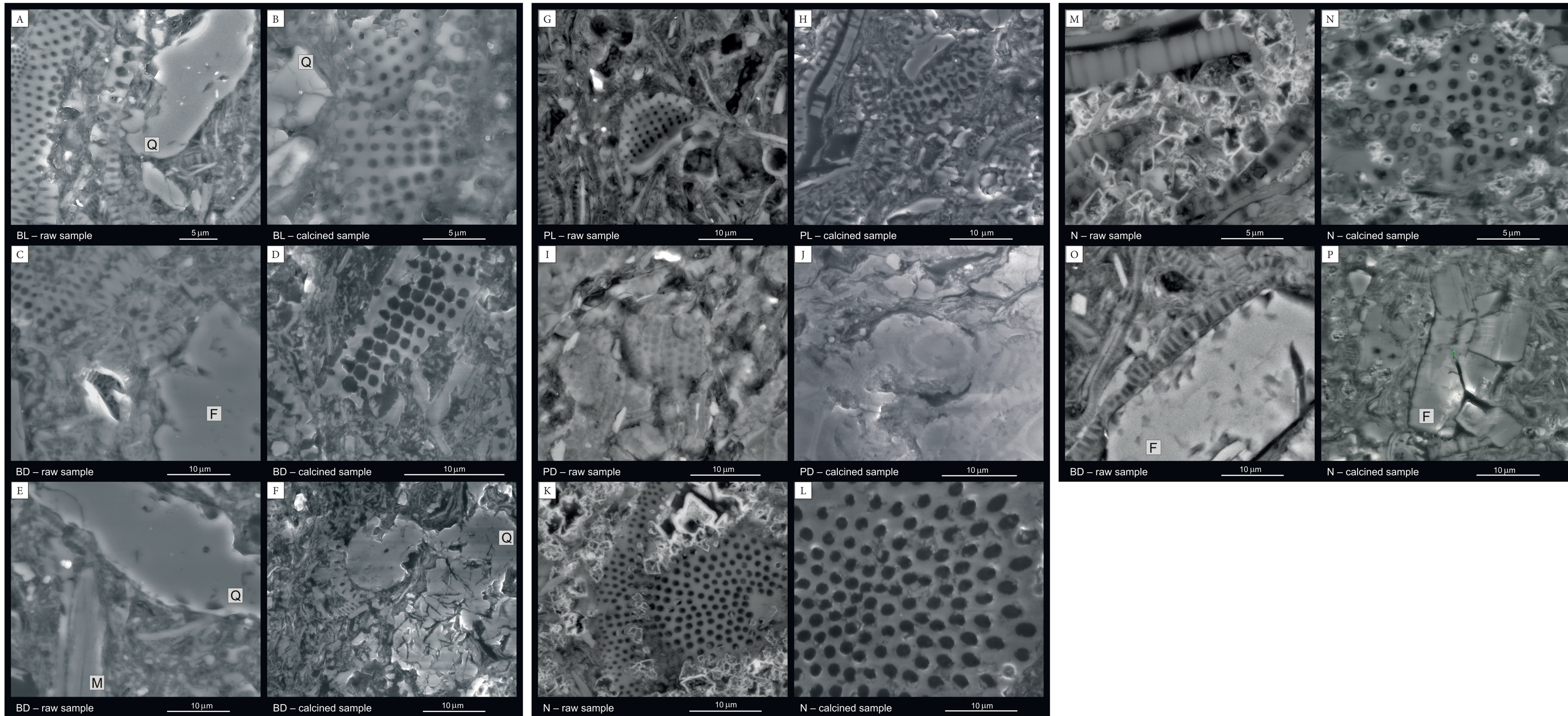
Fig. 2. *SEM micrographs of the Jawornik diatomaceous rocks: Q – quartz, F – feldspar, M – micas (explanations A–P in the text)*

The list of the groundmass components is completed with fragments of organic substances: 1–2% in the BL, PL and PD varieties and 4–5% in the BD and N ones (Figarska-Warchoł et al. 2015).

In SEM observations, the diatomites are characterized by highly complex, mutually connected intergranular and intragranular pores (Fig. 2A, C, G). The intergranular pores are numerous and of irregular shapes that results from a random arrangement of the groundmass and framework components with various habits. Pore sizes usually do not exceed 5 μm. Only in the PD variety are the intergranular pores more common, which is due to an abundant silica that has cemented framework components into compact, randomly arranged zones (Fig. 2I). In the diatomites of most varieties (except variety PD) large cavities commonly occur within the frustules, sometimes filled with clay minerals, organic substance or iron oxy/hydroxides, occasionally with silica (Fig. 2G). They reach 30 μm and have regular shapes (spherical, cylindrical or tubular), disturbed when the diatom shells are crumbled into smaller fragments. Also abundant are spherical, fine pores with diameters 100–1500 nm (usually below 400 nm), located within the frustules. Usually they are arranged regularly and this distribution is a characteristic feature of individual taxa of diatoms (Fig. 2A, K). In some of the diatoms, particularly in the PD variety, such pores and also the interiors of the shells are partly or completely filled with amorphous silica.

The chemical composition of the diatomites is closely related to the mineral phases specified above. Their silica contents are not too high: from ca. 60% (variety N) to ca. 75–80% (BL, BD and PL) and to ca. 85% SiO_2 (PD). The minor chemical compounds include: alkalis (attributed mainly to feldspars) that range from ca. 1% (PD) to above 2% $Na_2O + K_2O$ (PL), 1–5% Fe_2O_3 (attributed to iron oxide/hydroxides) (with the variety N being an exception as it contains above 17% Fe_2O_3) and ca. 7–10% LOI (attributed to the presence of an organic substance and to the water expelled from the hydrated forms of silica) (Figarska-Warchoł et al. 2015).

METHODS

From each of the five distinguished lithological varieties of the diatomites, three irregular lumps with the mass 20–60 g each were taken. Thermal treatment was applied to change the structural properties of the diatomites, mainly to increase their porosity and water absorbability, with a simultaneous improvement of their mechanical strength. Therefore, the samples were calcined in a laboratory furnace at 600°C in the ambient air. The literature results indicated that such a calcination temperature slightly exceeds the temperature of the structural transition from β and α quartz (573°C), simultaneously being considerably lower than the temperatures of significant alterations of other minerals. During such a calcination, the surface-bound water and an organic substance should be removed, whereas clay minerals dehydroxylated and partly decomposed (Yılmaz & Ediz 2008, Zhi-Yang et al. 2009, Ediz et al. 2010, Posi et al. 2014, Zheng et al. 2018). Melting of clay minerals in pores was also reported to start at 600°C (Zhi-Yang et al. 2009). These processes should strengthen the framework of the diatomites without lowering their porosity and specific surface (Sun et al. 2013). The furnace temperature was increased at the rate 20°C/min. in the range 20–150°C and then at 4°C/min. until the assumed 600°C was reached, and this calcination temperature was kept for the next 24 h. Finally, the samples were cooled for 48 h to reach room temperature.

The effects of calcination in the Jawornik diatomite varieties were analysed in thin sections under a scanning electron microscope and the mineral composition was identified with X-ray diffraction (XRD) on powder samples, while their physical properties and microhardness were determined prior and after the thermal treatment of irregular rock pieces.

Microscope observations were carried out in the laboratories of AGH UST to analyse the changes of shapes and sizes of mineral grains using FEI Quanta 200 FEG (low-vacuum) and FEI Company NOVA NANO SEM SEM microscopes, equipped with back scattered electron (BSE) detectors and EDS peripherals. XRD analyses helped to identify the mineral phases present in raw and calcined samples of diatomites of different varieties. An X-ray diffractometer DRON 3.0 was used applying the Debye-Sherrer powder method.

The essential rock properties, i.e., the water absorption and apparent density, were determined

following the European standards EN-13755:2008 and EN-1936:2006. Subsequently, the mercury porosimetric tests were carried out in an AGH UST laboratory using a PASCAL 140/240/440 ver. 1.01 mercury porosimeter made by CE Instruments. They were based on the volume of mercury pressure-injected into the pore space of the rocks. At the pressures ranging between 0.10 and 150 MPa, mercury could penetrate cylindrical capillaries with the smallest diameters ca. 0.01 μm. The following structural parameters of the pore spaces of the diatomites were determined: the distribution of pore diameters, including macropores with the diameters $d > 100$ nm and $d > 50$ nm, the average pore-throat diameter, the specific pore surface area and the total rock porosity (Klobes et al. 2006).

The resistance of the diatomites to the stress exerted by point-acting outer pressure was given as their microhardness (HV). The measurements were conducted using a Testlab HVKD-1000IS hardness tester with a pyramidal diamond indenter (the Vickers method). The hardness was expressed as a quotient of the indenter load (0.3 kgf = 2,942 N) and the side surface of the pyramidal indentation, calculating the latter from the length of the diagonals of indentation marks (Winkler 1997). For each sample, 20–30 measurements were carried out spaced at a distance of 1 mm along 1 or 2 lines to obtain the randomness of the $HV_{0.3}$ data. These measurements were used for calculating the arithmetical mean and standard deviation values.

RESULTS OF CALCINATION

Mineral composition and structural properties

The XRD analyses and the SEM observations of the calcined diatomites indicate that the temperature of 600°C caused changes of various intensity and character in the rock structure, depending on the initial mineral composition and structural features of the specified rock varieties.

The amount of amorphous silica increased with heating, as proven by the elevated backgrounds on the X-ray patterns in the range 15–40° 2θ, while the intensities of quartz reflections distinctly decreased (Fig. 3). These changes are expressed mainly in the **BL, PL** and **N varieties**, and the weakest in the **PD** and **BD varieties**.
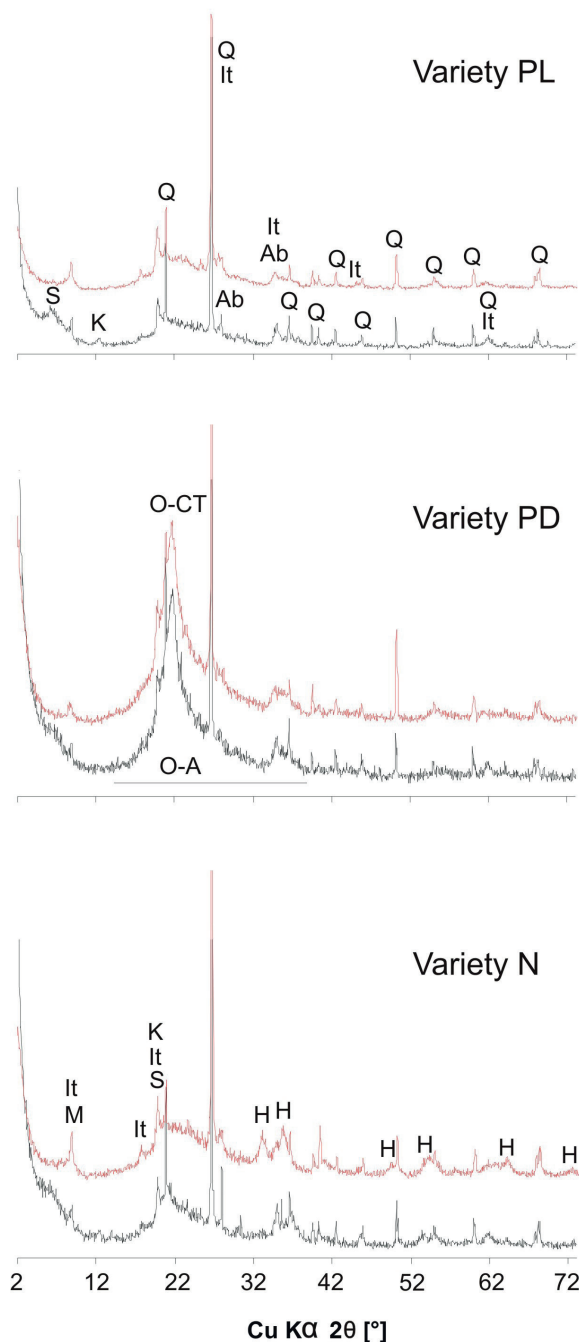

Fig. 3. *Comparison of X-ray diffraction patterns of three diatomite varieties obtained for raw (black lines) and calcined (red lines) samples. Explanations: Q – quartz, O-A – opal-A, O-CT – opal-CT, It – illite, S – smectite or mixed-layered illite-smectite, K – kaolinite, Ab – albite, M – micas, H – hematite*

In the X-ray patterns of all the diatomite types the reflections of kaolinite and smectites either disappeared or considerably decreased their intensities, while the reflections of illite were stronger. It is

best pronounced in the **BL, PL** and **N varieties** and weaker in the **BD** and **PD** ones (Fig. 3). A change of the intensities of the overlapping reflections of illite and albite also indicate a decrease of the latter.

In case of the **N variety,** the major reflections of hematite were stronger, while several additional weak ones appeared after calcination.

The changes described above are represented in the triangular diagram, distinguishing the total of amorphous silica that forms frustules and the diatomite background (50–80%), the detrital quartz (3–9%), and the total of clay minerals plus feldspar grains. The diagram also shows the approximate directions and intensities of the changes of the mineral transformations recorded on heating the diatomites at 600°C (Fig. 4).

Signs of the initial melting of thin frustules were expressed as an increase of the diameters of their larger pores (Fig. 2D, H) or a decrease of the finer ones – filled with melting products, mostly with amorphous silica (Fig. 2B, N). The processes of melting caused the pore borders to be irregular and fray-like, while the pore shapes often became elongated (Fig. 2D, L). These pore features differ sharply from those of the pores prior to calcination: the initial pores were spherical and their borders smooth (Fig. 2G, K). The enlargement of the frustule pores resulted in lowering the thickness of the walls that separate the pores from one another (Fig. 2D, H, L). Extensive melting of the PL variety made it more spongy (Fig. 2H). The effects of calcination in the PD variety differed from those described earlier, because the PD diatomites are highly coherent. The pores in their frustules, already filled with silica prior to calcination (Fig. 2I), were not enlarged, but the ornamentation of the diatoms became even more obscured (Fig. 2J). In the rocks of the N variety, calcination resulted in the weak melting of the diatoms and therefore only a few pores were enlarged (Fig. 2L).

The thinning of the pore walls favoured their cracking and, as a result, the fractures joined neighbouring pores (Fig. 2H, L). In the case of thicker frustule fragments, the pores had not been enlarged during calcination, but heating resulted in the formation of single fractures that extend through the whole diatom shell (i.e. continue on the other side of the pore) and divide frustules into small fragments (Fig. 2B, N).

Many of the grains of quartz and feldspars were fractured and also disintegrated. This process began on the grain surfaces and was observed as fine cavities of irregular shapes in quartz and triangular in feldspars. In the grains exposed to elevated strain induced by their thermal enlarging, the splintering was accompanied by cracking. The fractures are irregular in quartz and mutually intersect (Fig. 2B, F), whereas in feldspars their linear arrangement follows the oblique cleavage typical of these minerals (Fig. 2P). Such phenomena occurred less often prior to calcination (Fig. 2A, C, E, O).

It was also observed that the groundmass structure of the diatomites was partially sealed, perhaps because the smallest pores among clay flakes were filled with the products of decomposing clay minerals (their flakes are weakly visible in the samples after calcination) (Fig. 2B, H) and/or with silica generated by melting of fine detrital diatom grains.

The grains of iron oxides/hydroxides, unusually common in diatomite of the N variety, distinctly changed their habits. Their idiomorphic outlines, sometimes even rectangular or rhombohedral (Fig. 2M), became oval or irregular and their sizes slightly decreased (Fig. 2N).
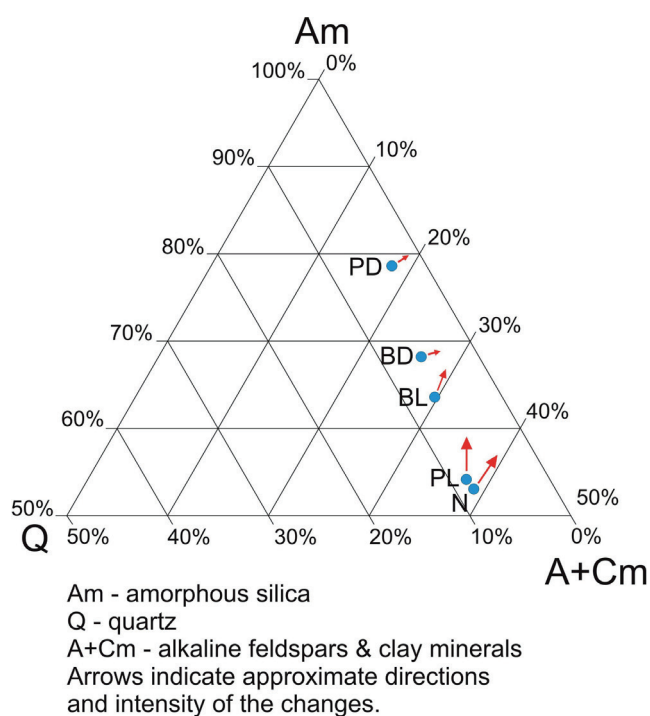

Am - amorphous silica
Q - quartz
A+Cm - alkaline feldspars & clay minerals
Arrows indicate approximate directions
and intensity of the changes.

Fig. 4. *Contents of main diatomite components in raw samples with approximate directions and intensities of their changes after calcination*

The SEM observations are insufficient to unambiguously identify the effects of the oxidation of the organic matter, whose amounts reach 5% in the raw diatomites. As the organic matter burns well below 600°C, it can be assumed that this process formed part of the fine pores of the calcined diatomites.

Physical properties

The determination of physical rock properties corroborates a known, highly correlated ($R^2 = 0.87$) relation between water absorbability and apparent density. Of the raw, not calcined diatomite samples, the highest values of water absorbability, close to 30%, are to be found in the BL and N varieties, medium ones, ca. 20%, in the BD and PL varieties, and the lowest ones, ca. 12%, in the PD variety (Tab. 2). The apparent density values ranged from 1.28 g/cm³ to 1.77 g/cm³. In all the varieties, calcination increased water absorbability and decreased density. The highest increase of the first parameter is noted in the samples of the BD – 7.65% and N varieties – 5.22%, whereas in the light-coloured diatomites with the blocky disintegration of the variety BL the growth was only 0.9%.

More precise determinations using mercury pressure porosimetry prove that uncalcined diatomites with blocky disintegration (variety BL) and nodular disintegration (variety N) have the lowest apparent densities and, at the same time, the highest total porosities (ca. 38–40%) (Tab. 3).

Table 2
Water absorption and apparent density of the Jawornik diatomites

Diatomite variety	Water absorption by mass [%] average minimum – maximum		Apparent density [g/cm³] average minimum – maximum	
	raw	calcined	raw	calcined
BL	31.01 30.61–31.42	31.91 31.66–32.16	1.28 1.27–1.29	1.25 1.24–1.26
BD	20.17 18.42–21.91	27.82 24.44–31.21	1.47 1.42–1.52	1.36 1.27–1.46
PL	22.97 22.61–23.32	25.91 23.91–27.90	1.47 1.46–1.47	1.39 1.35–1.43
PD	12.67 12.53–12.74	15.01 14.97–15.07	1.77 1.69–1.94	1.62 1.61–1.62
N	29.26 –	34.48 –	1.41 –	1.34 –

Table 3
Mercury porosimetry data of the Jawornik diatomites (results for raw samles / calcined samples)

Diatomite variety	Total porosity* [%]	Average pore-throat diameter [nm]	Total specific surface area [m²/g]	Content of the macropores (diameter >50 nm) [%]	Content of the macropores (diameter >100 nm) [%]
BL	37.99/42.15	181.6/650.0	13.5/10.3	87.30/91.62	65.63/81.92
BD	33.34/37.86	130.2/100.0	15.1/15.3	78.86/84.48	53.63/55.27
PL	25.92/36.49	117.4/116.0	5.0/13.7	86.84/84.88	75.69/46.42
PD**	2.57/8.79	13.0/26.0	3.0/8.1	25.80/17.60	15.72/4.20
N	40.10/43.88	181.4/760.0	14.8/14.0	83.61/87.00	65.94/72.20

 * total porosity calculated using the results of mercury porosimetry,

** raw sample damaged at a pressure of around 100 MPa.

The average pore-throat diameter is ca. 180 nm, and the contributions of all macropores (i.e. those with diameters above 50 nm) are 87.30% and 83.61%, respectively. Similar contributions of the macropores occur in the PL and BD varieties, but both their total porosities and the average pore-throat diameters are lower than those of the BL and N varieties. The PD variety has its pores with an average diameter of only 13 nm, while the contribution of macropores ($d > 50$ nm) is low and amounts to 25.80%. Such pores could hardly be penetrated by mercury, thus the total rock porosity is low (2.57% – Tab. 3).

The distribution of pore sizes in the raw samples of the BL, BD and N varieties is relatively similar. The most abundant are the pores with the diameters 100–250 nm, while the contributions of the pores >400 nm are negligible (Fig. 5). The largest pores reach diameters of 10,000–12,000 nm. The calcination of these three rock varieties increased the relative contribution of the larger pores, i.e. those with the diameters to 800 nm in the diatomites with the blocky disintegration (BL and BD) and to 1000 nm in the variety with the nodular disintegration (N).

The pore space of the raw diatomites of the PL variety is characterized by a high differentiation of pore sizes in the diameter range 10–4000 nm, with the contribution of the pores with diameters >700 nm being slightly higher than those of the finer pores (Fig. 5). The calcination of this variety increased the relative contribution of the pores with diameters 50–200 nm significantly, whereas the relative contribution of the mesopores in the range 10–50 nm remained at the same level, while the macropores with the diameters 200–2000 nm disappeared. However, the content of the largest macropores with diameters 2000–10,000 nm is significant.

The pore distribution in the PD variety stands in contrast to that of the PL variety. The finest pores with the diameters 10–12 nm dominate in the raw diatomites of this type: they can be classified as intermediate between micro- and mesopores (Fig. 5). The contribution of the pores <200 nm is significant, while the diameters of the largest pores reach 3000 nm. Calcination clearly lowered the contribution of the finest pores and significantly increased the contribution of the pores with the diameters 20–100 nm. The pores with the diameters 1000–4000 nm and 6000–12,000 nm occur occasionally.
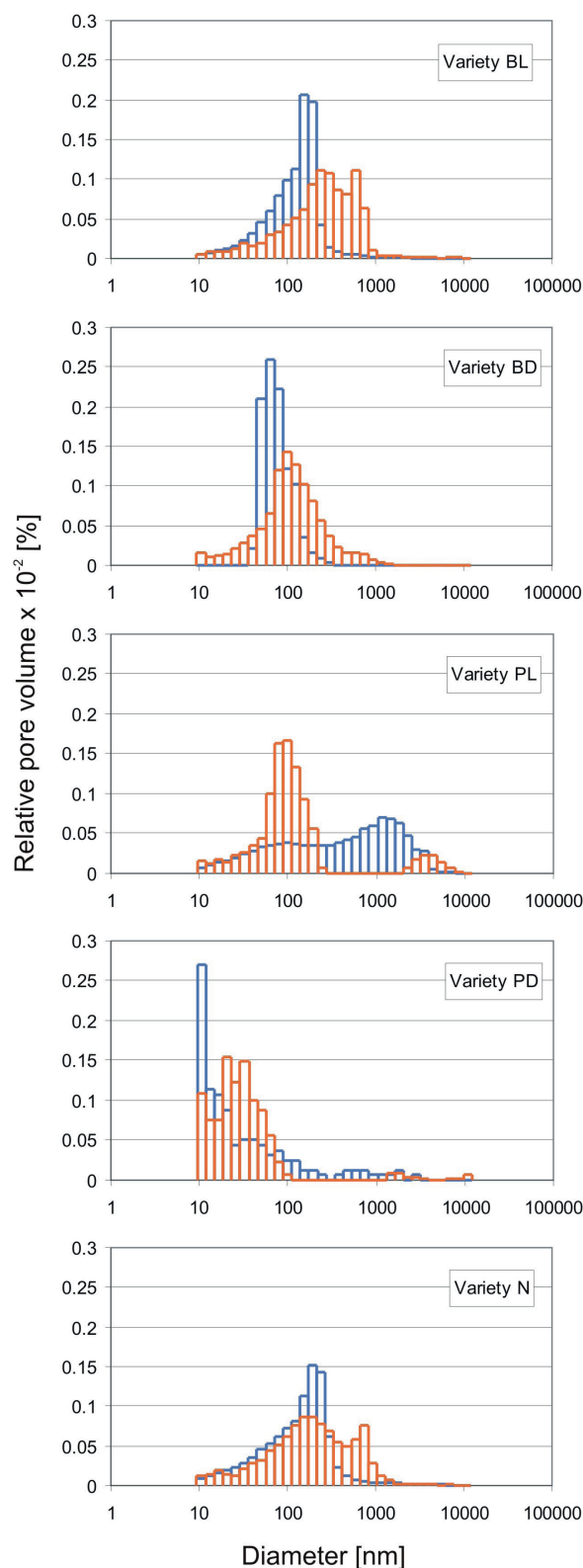

Fig. 5. Pore volume distributions in raw (blue bars) and calcined (red bars) Jawornik diatomites

Microindentation hardness

The raw diatomite samples are characterized by relatively low microhardness, not exceeding 25 MPa, except the PD variety, whose microhardness exceeds 92 MPa (Tab. 4). Particularly low are the microhardness values of the light-coloured BL and PL diatomite varieties and of the diatomites with the nodular disintegration (variety N).

Calcination increased microhardness in all of the diatomites, mostly in the varieties PL (the relative increase by 109.4%) and BD (the relative increase by 40.4%). The microhardness values of the soft diatomites BL and N increased by a mere 2–3 MPa, which makes ca. 23–25% of this parameter in the samples prior to calcination. The structure of the most compact variety, PD, was strengthened and its microhardness has reached 100 MPa.

Table 4
Vickers microhardness values of the Jawornik diatomites

Diatomite variety	$HV_{0.3}$ [MPa]	Range	Standard deviation	$HV_{0.3}$ [MPa]	Range	Standard deviation	Relative increase of microhardness [%]
	Raw samples			Calcined samples			
BL	8.4	4.3–12.6	2.0	10.3	5.7–17.1	2.5	+22.7
BD	23.2	15.7–26.6	3.3	32.6	26.6–40.9	4.0	+40.4
PL	9.2	7.6–11.5	1.1	19.2	16.2–21.6	1.7	+109.4
PD	92.2	76.3–122.4	12.5	99.9	81.9–127.6	12.3	+8.4
N	10.5	6.2–14.1	2.1	13.1	9.3–18.1	2.1	+25.1

DISCUSSION

Calcination of the Jawornik diatomites at 600°C initiated a range of processes. The most important were: transformations of various silica forms, phase and physical changes of other minerals, and also oxidation of the organic matter. They ran concurrently and induced physical and mechanical changes to the diatomites tested. The intensity of these changes depended on the initial rock composition and the structure of diatomite varieties.

An **incipient melting of siliceous mineral components** was one of the major processes observed in the SEM analyses and confirmed in the XRD investigations. The relative increase of the amorphous silica content (high XRD background) was accompanied by a respective decrease in the quartz content (quartz XRD reflections were weaker) (Fig. 3). Incipient melting can also be traced in SEM images: larger pores of the diatom fossils increased their diameters (Fig. 2D), while smaller pores became finer after being filled with the melted silica (Fig. 2B, J). It may be assumed that the finest fragments of the diatoms, as well as part of the silica in the rock background, melted at 600°C. There are no undiscutable melting signs of larger quartz grains, but it is possible that melting might have affected their finest fractions.

Clay minerals were **dehydrated and dehydroxylated** on heating to 600°C, and especially the latter process might have remained unfinished depending on the composition of the clay minerals (Stoch 1974). The presence of some mineral phases may have caused the **transformation of the clay minerals into amorphous phases** (Zhi-Yang et al. 2009), providing an additional source of alkalis (most of the alkalis were derived from feldspars). In ceramics, the alkalis lower the melting temperatures of the ceramic charge, therefore the presence of Na_2O and K_2O could have also initiated the melting of the Jawornik diatomites already below 600°C.

Another effect of calcination was caused by the **shrinking and expanding of mineral grains**. Clay mineral flakes most probably shrank during dehydration below 200°C, but when temperature increased the linear sizes of the clay flakes also increased, and around 600°C they shrank again due to dehydroxylation. Dehydration at low temperatures must have also reduced the volume of other mineral components consisting of opal, mainly diatoms. The polymorphic transformation of quartz β into quartz α, also associated

with enlarging the size of quartz grains, took place at 573°C (Stoch 1974). Other grain components, for instance feldspars, probably enlarged their sizes, too.

Fracturing of quartz and feldspar grains observed in SEM images (Fig. 2B, F, P) was generated by the process of the linear expansion of minerals characterized by a high specific heat, when their porous, mother rocks with a low thermal conductivity are heated. According to Germanovich (1997) and Deeny et al. (2009), such conditions form local compression centers within the hot, outer parts of minerals. As a result, the expanding minerals and some of their fragments splinter off (Rauenzahn & Tester 1989). Quartz is particularly prone to such thermal processes. According to Robertson (1988), the coefficient of thermal expansion of quartz is relatively high between 20°C and 400°C, being $4.98 \cdot 10^{-5} \cdot K^{-1}$, while that of albite $(2.24 \cdot 10^{-5} \cdot K^{-1})$ is almost two times lower.

Thermal expansion also favoured the **cracking of the frustule walls** between expanding pores (Fig. 2B, H, L), as well as initiating the **formation of large cavities** among mineral components or extending the size of existing hollows (Fig. 2J).

A certain increase in the porosity of the calcined diatomites may also be attributed **to the presence of dispersed organic matter**, whose amounts range between ca. 1.0% and 3.5%. The carbonized organic matter simply disappears during heating in the air as CO_2 (the effect of oxidation) and cannot be detected in SEM images. The process was accompanied by the change of colours of the diatomites from grey in the raw samples, to light creamy with a pink tint after calcination. The pink colour indicates the admixture of oxidized iron-containing mineral components in the diatomites, and was corroborated by hematite reflections identified in the X-ray patterns of the N diatomite variety.

The processes described above mark the complex picture of structural and mineral changes of the Jawornik diatomites. Due to them, these rocks also changed in terms of some of their technological properties.

The highest degree of amorphization was revealed in the calcined PL, N and BL varieties (Fig. 4). These raw diatomites contained relatively low amounts of amorphous silica (Am: 53–64%)

and were considerably rich in clay minerals, micas and feldspars (A+Cm: 30–39%). The content of clay minerals themselves was the highest in the PL variety (above 31%), the rock in which the increase of porosity was also the highest (by 10.6%) with a simultaneous decrease of the nanopores larger than 500 nm. The porous system of the PL variety also developed on heating as its specific surface area is higher by 8,7 m²/g (174%), while the content of smaller pores in the range 50–170 nm increased (Fig. 5). Such results depend not only on the high content of clay minerals, but also on a strong fragmentation of the diatoms: the fine diatom remnants could have been melted easier than the large ones. Cementation of the rock groundmass by amorphous substances led to the highest relative increase in microhardness of all the samples, by as much as 109.4%, while a simultaneous lowering of the content of clay minerals improved porosity, an important structural rock parameter.

The process of melting silica mainly caused the increase of pore diameters in diatom frustules in the BL and N varieties, which differed from the types described above in terms of their considerably higher content of undamaged diatoms. Moreover, numerous cracks of diatoms and other grains led to the increase in the volume of the largest pores (Fig. 5). It was confirmed by substantial increase of average pore-throat diameters (to over 400 nm) and a lowering of the total specific surface area (Tab. 3). On the other hand, the filling of some pores with the products of melting and iron oxydation (hematite) observed in SEM images, as well as the expected disappearance of fine accumulations of organic matter, did not change the relative content of finest pores. The cementation of groundmass components, similar to the PL variety, triggered a considerable relative increase in microhardness (over 20%).

The BD and PD varieties in the raw state contained high amounts of amorphous silica (Am: 68% and 79%, respectively), which was accompanied by low contents of clay minerals and feldspars (A+Cm: 26% and 18%, respectively). On the one hand, calcination brought about minor changes in the ratio between the contents of amorphous silica and quartz, and opal-CT on the other. The finer pores prevailing in the rock were either widened (BD variety), or filled and blocked

(PD variety). Fracturing on heating was higher in the BD variety than in the PD, and the latter one was more homogenous considering both its mineral composition and structure. Therefore, the mechanical resistance of these rocks, expressed as microhardness, increased distinctly by ca 40% in the BD variety and only by 3.4% in the coherent PD one (Tab. 4).

CONCLUSIONS

The effectiveness of the calcination of Jawornik diatomites at 600°C is differentiated, mainly because of the various mineral composition of the five rock varieties distinguished, and, to a leseer extent, of their varying structures and textures. Obtaining an increase of the overall rock porosity was the major aim of the experiments. This can be achieved by increasing the internal pores of the frustules due to their incipient melting, thermal fracturing of the frustule walls and of the grains of other diatomite components (feldspars, quartz). The porosities also grow due to the lowering of the volumes of clay minerals and opal, which dehydrate and dehydroxylate on heating, and, to a lesser degree, to oxidating organic matter. The distribution of the pores also changed after calcination within the whole range of diameters.

In the rock varieties with the highest initial porosities, i.e. BL (diatomites with blocky disintegration) and N (diatomites with nodular disintegration), calcination imparted the most intensive development of macropores, expressed by both the increase of their contents and a considerable increase of their pore-throat diameters. These phenomena were accompanied by the lowering of specific surface values. In the variety with low initial porosity, and also in which diatomite fossils were considerably fragmented (PL), the processes of mineral transformations resulted in the higher development of pores with diameters of 70–130 nm and a relative lowering of the macropore content. Such a distribution of pore sizes is advantageous to the increase of porosity and specific surface area.

The phenomena of tranforming and deforming mineral components exposed to heating at 600°C also increased the microhardness of the diatomites of all varieties. This change depends significantly on the rock content of clay minerals

($r^2 = 0.85$), which dehydrate and dehydroxylate during calcination. Therefore, microhardness increased mostly in the rock variety PL, which is the richest in clay minerals. Other mineral components have no impact on microhardness after calcination. With regard to the diatomite structure, calcination increased rock microhardness most in the soft and porous rocks, while only to a limited extent in the hard and compact varieties. Therefore, the microhardness differences distinct in the raw diatomites were partly reduced after heating.

The process of the calcination of diatomites differing in their technological properties has resulted in obtaining mineral material with a porosity exceeding 36% and microhardness $HV_{0.3}$ in the wide range 13.1–99.9 MPa. The processed diatomites revealing such properties may be used in the production of deiceing and antisliding road aggregates. The technology of their manufacture has been covered by patent protection (the patent application No. P-429759) and attempts at its industrial implementation have been initiated. Other industrial applications of Jawornik diatomites may include only selected rock varieties whose calcination will provide mineral raw materials with porosity and microhardness values which differ in narrow ranges.

REFERENCES

Abrantes F., Lopes C., Mix A. & Pisias N., 2007. Diatoms in Southeast Pacific surface sediments reflect environmental properties. *Quaternary Science Reviews*, 26, 155–169.

Aruntaş H.Y., Albayrak M., Saka H.A. & Tokyay M., 1998. Investigation of diatomite properties from Ankara-Kızılcahamam and Çankırı-Çerkeş regions. *Turkish Journal of Engineering and Environmental Sciences*, 22, 337–343.

Cummins A.B., 1973. Development of diatomite filter aid filtration. *Filtration and Separation*, 10, 2, 215–219.

Deeny S., Stratford T., Dhakal R.P., Moss P.J. & Buchanan A.H. 2009. Spalling of concrete: implications for structural performance in fire. [in:] Wald F., Kallerová P.,

Chlouba J. (eds.), *Proceedings of International Conference in Prague, 19–20 February 2009*: Applications of Structural Fire Engineering, Czech Technical University in Prague, Prague, 202–207.

Ediz N., Bentli İ. & Tatar İ., 2010. Improvement in filtration characteristics of diatomite by calcination. *International Journal of Mineral Processing*, 94, 129–134.

EN-13755:2008. *Natural stone test methods – Determination of water absorption at atmospheric pressure*. CEN European Committee for Standarization.

EN-1936:2006. *Natural stone test methods – Determination of real density and apparent density, and of total and open porosity*. CEN European Committee for Standarization.

Figarska-Warchoł B., Stańczak G., Rembiś M. & Toboła T., 2015. Diatomaceous rocks of the Jawornik deposit (the Polish Outer Carpathians): petrophysical and petrographical evaluation. *Geology, Geophysics & Environment*, 41, 4, 311–331.

Fustinoni S., Campo L., Colosio C., Birindelli S. & Foa V., 2005. Application of gas chromatography-mass spectrometry for the determination of urinary ethylenethiourea in humans. *Journal of Chromatography B: Analytical Technologies in the Biomedical and Life Sciences*, 814, 2, 251–258.

Fuya W., Huifen Z., Huang F., Guoxi C., Deqiang W. & Hongping H., 1995. A mineralogical study of diatomite in Leizhou Peninsula. *Chinese Journal of Geochemistry*, 14, 140–151.

Gao B., Jiang P., An F., Zhao S. & Ge Z., 2005. Studies on the surface modification of diatomite with polyethyleneimine and trapping effect of the modified diatomite for phenol. *Applied Surface Science*, 250, 273–279.

Germanovich L.N., 1997. Thermal Spalling of Rocks. [in:] Karihaloo Bhushan L. (ed.), *Advances in fracture research: proceedings of the Ninth International Conference on Fracture; 1 – 5 April 1997, Sydney, Australia*, Pergamon, Amsterdam, 2771–2782.

Goren R., Baykara T. & Marsoglu M., 2002. Effects of purification and heat treatment on pore structure and composition of diatomite. *British Ceramic Transactions*, 101, 177–180.

Haluska M.S., Dragomir-Cernatescu I.C., Sandhage K.H., & Snyder R.L., 2005. X-ray diffraction analysis of 3-D MgO diatom replicas synthesized by low-temperature gas/solid displacement reaction. *Powder Diffraction*, 20, 4, 306–310.

Hassan M.S., Ibrahim I.A. & Ismael I.S., 1999. Diatomaceous deposits of Fayium, Egypt: Characterization and evaluation for industrial application. *Chinese Journal of Geochemistry*, 18, 233–241.

Ibrahim S.S. & Selim A.Q., 2010. Producing a micro-porous diatomite by a simple classification-calcinations process. *The Journal of Ore Dressing*, 12, 23, 24–32.

Jucha S. & Kotlarczyk J., 1961. *Seria menilitowo-krośnieńska w Karpatach fliszowych*. Prace Geologiczne PAN, Oddział w Krakowie, Komisja Nauk Geologicznych, 4, Wydawnictwa Geologiczne, Warszawa.

Khraisheh M.A.M., Al-Ghouti M.A., Allen S.J. & Ahmad M.N., 2005. Effect of OH and silanol groups in the removal of dyes from aqueous solution using diatomite. *Water Research*, 39, 922–932.

Klobes P., Meyer K. & Munro R.G., 2006. *Porosity and specific surface area measurements for solid materials*. NIST Recommended Practice Guide, NIST Special Publication, 960, 17, U.S. Department of Commerce, Technology Administration, National Institute of Standards and Technology.

Koszarski L. & Żytko K., 1961. Łupki jasielskie w serii menilitowo-krośnieńskiej w Karpatach środkowych [Jasło Shales within the Menilite-Krosno Series in the Middle Carpathians]. *Biuletyn Instytutu Geologicznego*, 166, 87–232.

Kotlarczyk J., 1955. O występowaniu diatomitu we fliszu Karpat polskich. *Przegląd Geologiczny*, 5, 244.

Kotlarczyk J., 1966. Poziom diatomitowy z warstw krośnieńskich na tle budowy geologicznej jednostki skolskiej w Karpatach polskich. *Studia Geologica Polonica*, 19, 1–129.

Kotlarczyk J., 1982. The role of diatoms in sedimentation and biostratigraphy of the Polish Flysch Carpathians. *Acta Geologica Academiae Scientiarum Hungaricae*, 25, 1–2, 9–21.

Kotlarczyk J., 1988a. Jawornik Ruski – kopalnia diatomitu. Poziom diatomitów z Leszczawki, najmłodsza olistostroma we fliszu. [in:] Kotlarczyk J., Pękala K. & Gucik S. (red.), *Karpaty przemyskie: przewodnik LIX Zjazdu Polskiego Towarzystwa Geologicznego, [Przemyśl] 16-18 września 1988*, Wydawnictwa AGH, Kraków, 115–118.

Kotlarczyk J., 1988b. Poziom diatomitów z Leszczawki. Punkt B-3. Jawornik Ruski. 1. Geologia i własności surowca. [in:] Kotlarczyk J., Pękala K. & Gucik S. (red.), *Karpaty przemyskie: przewodnik LIX Zjazdu Polskiego Towarzystwa Geologicznego, [Przemyśl] 16-18 września 1988*, Wydawnictwa AGH, Kraków, 149–154.

Kotlarczyk J., Brożek M. & Michalski M., 1986. Diatomity polskich Karpat – występowanie, jakość, przeróbka i zastosowania. *Gospodarka Surowcami Mineralnymi*, 2, 3–4, 497–523.

Kotlarczyk J. & Leśniak T., 1990. *Dolna część formacji menilitowej z poziomem diatomitów z Futomy w jednostce skolskiej polskich Karpat*. Wydawnictwa AGH, Kraków.

Li X., Li X. & Wang G., 2007. Surface modification of diatomite using polyaniline. *Materials Chemistry and Physics*, 102, 140–143.

Malata T., 1996. Analiza formalnych wydzieleń litostratygraficznych oraz propozycja podziału jednostki skolskiej polskich Karpat fliszowych. *Przegląd Geologiczny*, 44, 5, 509–513.

Malata T. & Poprawa P., 2006. Ewolucja subbasenu skolskiego. [in:] Oszczypko N., Uchman A. & Malata E. (red.), *Rozwój paleotektoniczny basenów Karpat zewnętrznych i pienińskiego pasa skałkowego*, Instytut Nauk Geologicznych Uniwersytetu Jagiellońskiego, Kraków, 103–110.

Marcinowski R., Mardal R. & Piotrowska K., 2011. *Słownik jednostek litostratygraficznych Polski. Wersja podstawowa (grudzień 2004–2011)*. PIG, [on-line:] http://slp.pgi.gov.pl/index.php [October 2013].

Martinovic S., Vlahovic M., Boljanac T. & Pavlovic L., 2006. Preparation of filter aids based on diatomites. *International Journal of Mineral Processing*, 80, 255–268.

Mohamedbakr H. & Burkitbaev M., 2009. Elaboration and characterization of natural diatomite in Aktyubinsk/Kazakhstan. *Open Mineralogy Journal*, 3, 12–16.

Murer A., McClennen K., Ellison T., Timmer R., Larson D., Wolcott K., Walker T., Thomsen M. , 2000. Steam injection project in heavy-oil diatomite. *SPE Reservoir Evaluation & Engineering*, 3, 2–12.

Obanijesu E.O., Bello O.O., Osinowo F.A.O. & Macaulay S.R.A., 2004. Development of a packed-bed reactor for the recovery of metals from industrial wastewaters. *International Journal of Environment and Pollution*, 22 (6), 701–709.

Oszczypko N., 2008. Outher Carpathians in Poland. [in:] McCann T. (ed.), *The Geology of Central Europe. Volume 2: Mesozoic and Cenozoic*, Geological Society, London, 1078–1081.

Posi P., Lertnimoolchai S., Sata V., Phoo-ngernkham T. & Chindaprasirt P., 2014. Investigation of properties of lightweight concrete with calcined diatomite aggregate. *KSCE Journal of Civil Engineering*, 18, 5, 1429–1435.

Rauenzahn R.M. & Tester J.W. 1989. Rock failure mechanisms of flame-jet thermal spallation drilling – theory and experimental testing. *International Journal of Rock Mechanics and Mining Sciences*, 26, 381–399.

Robertson E.C. 1988. *Thermal properties of rock. United States Department of The Interior, Geological Survey.* Open-File Report 88–441, United States Department of the Interior Geological Survey.

Russocki Z., 1981. Zmienność diatomitów w złożu Leszczawka. [in:] Szymańska A. (red.), *Nowe kierunki zastosowań diatomitów polskich w gospodarce narodowej: konferencja naukowo-techniczna, Przemyśl, 23–24 maja 1980*, Wydawnictwa Geologiczne, Warszawa, 30–40.

Sandhage K.H., Dickerson M.B., Huseman P.M., Caranna M.A., Clifton J.D., Bull T.A., Heibel T.J., Overton W.R. & Schoenwaelder M.E.A., 2002. Novel, Bioclastic route to self-assembled, 3-D, chemically tailored meso/ nanostructures: shape-preserving reactive conversion of biosilica (diatom) microshells. *Advanced Materials*, 14, 6, 429–433.

Smoleńska A. & Rembiś M., 2002. Diatomit jako lekkie kruszywo mineralne w tynkach renowacyjnych. [in:] *Kruszywa mineralne: surowce, rynek, technologie, jakość: Polanica Zdrój 17–19 kwietnia 2002*, Prace Naukowe Instytutu Górnictwa Politechniki Wrocławskiej, 97. Konferencje, 33, Oficyna Wydawnicza PW, Wrocław, 197–203.

Stańczak G., Rembiś M., Figarska-Warchoł B. & Toboła T., 2015. Fractal characteristics of the pore network in diatomites using mercury porosimetry and image analysis. [in:] Polychroniadis E.K., Oral A.Y. & Ozer M. (eds.), *2ⁿᵈ International Multidisciplinary Microscopy*

and Microanalysis Congress, Proceedings of InterM, October 16–19, 2014, Springer Proceedings in Physics, 164, Springer International Publishing, 79–89.

Stoch L., 1974. *Minerały ilaste*. Wydawnictwa Geologiczne, Warszawa.

Sun Z., Zhang Y., Zheng S., Park Y. & Frost R.L., 2013. Preparation and thermal energy storage properties of paraffin/calcined diatomite composites as form-stable phase change materials. *Thermochimica Acta*, 558, 16–21.

Szydło A., Garecka M., Jankowski L. & Malata T., 2014. Paleogene microfossils from the submarine debris flows in the Skole Basin (Polish and Ukraine Outer Carpathians). *Geology, Geophysics & Environment*, 40, 1, 49–65.

Toboła T., Rembiś M., Figarska-Warchoł B. & Stańczak G., 2015. Fibrous growth of chloride minerals on diatomite saturated with a brine. [in:] Polychroniadis E.K., Oral A.Y. & Ozer M. (eds.), *2nd International Multidisciplinary Microscopy and Microanalysis Congress, Proceedings of InterM, October 16–19, 2014*, Springer Proceedings in Physics, 164, Springer International Publishing, 73–78.

Winkler E.M., 1997. *Stone in Architecture: Properties, Durability*. 3 ed. Springer, Berlin.

Wu J., Yang Y.S. & Lin J., 2005. Advanced tertiary treatment of municipal wastewater using raw and modified diatomite. *Journal of Hazardous Materials*, 127, 196–203.

Xiong W. & Peng J., 2008. Development and characterization of ferrihydrite-modiffied diatomite as a phosphorus adsorbent. *Water Research*, 42, 4869–4877.

Yarusova S.B., Cherepanova M.V., Gordienko P.S. & Pushkar V.S., 2012. Sintez vollastonita iz prirodnogo dioksida kremniyai tekhnogennykh otkhodov. *Ekologiya i Promyshlennoct' Rossii*, 2, 24–27 [Ярусова С.Б., Черепанова М.В., Гордиенко П.С., Пушкарь В.С., 2012. Синтез волластонита из природного диоксида кремния и техногенных отходов. *Экология и промышленность России*, 2, 24–27].

Yılmaz B. & Ediz N., 2008. The use of raw and calcined diatomite in cement production. *Cement & Concrete Composites*, 30, 202–211.

Zheng R., Ren Z., Gao H., Zhang A. & Bian Z., 2018. Effects of calcination on silica phase transition in diatomite. *Journal of Alloys and Compounds*, 757, 364–371.

Zhi-Yang W., Li-Ping Z., Yu-Xiang Y., 2009. Structural investigation of some important Chinese diatomites. *Glass Physics and Chemistry*, 35, 6, 673–679.

Żgiet J., 1963. Spostrzeżenia nad sedymentacją wkładek diatomitów i tufów w Karpatach. *Kwartalnik Geologiczny*, 7, 714–715.